Small Molecule Targeting Malaria Merozoite Surface Protein-1 (MSP-1) Prevents Host Invasion of Divergent Plasmodial Species

Citation: Chandramohanadas, Rajesh; Basappa, Rajesh; Russell, Bruce; Liew, Kingsley; Yau, Yin Hoe; Chong, Alvin; Liu, Min et al. "Small Molecule Targeting Malaria Merozoite Surface Protein-1 (MSP-1) Prevents Host Invasion of Divergent Plasmodial Species." Journal of Infectious Diseases 210, no. 10 (May 2014): 1616–1626.

As Published: http://dx.doi.org/10.1093/infdis/jiu296

Publisher: Oxford University Press

Persistent URL: http://hdl.handle.net/1721.1/109166

Version: Author's final manuscript: final author's manuscript post peer review, without publisher's formatting or copy editing

Major Article

Running Title: Invasion Proteins as Drug Targets Against Human Malaria

Title: Small Molecule Targeting Malaria Merozoite Surface Protein-1 (MSP-1) Prevent Host Invasion of Divergent Plasmodial Species

Rajesh Chandramohanadas[#Ω], Basappa[#], Bruce Russell[¶], Kingsley Liew[#], Yin Hoe Yau[§], Alvin Chong[#], Liu Min[#], Karthigayan Gunalan[§], Rahul Raman[$], Laurent Renia[¥], Francois Nosten[‡ψ], Susana Geifman Shochat[§], Ming Dao[#†*], Ram Sasisekharan[#$], Subra Suresh[†] and Peter Preiser[#§*]

Author Affiliations:

Interdisciplinary Research Group of Infectious Diseases, Singapore MIT Alliance for Research & Technology Centre (SMART), Singapore-138602

Ω Singapore University of Technology & Design, 20 Dover Drive, Singapore- 138682

¶ Department of Microbiology, Yong Loo Lin School of Medicine, National University of Singapore, Singapore - 117545

§ School of Biological Sciences, Nanyang Technological University, Singapore- 637551

¥ Singapore Immunology network (SIgN), Agency for Science, Technology & Research (A*STAR), Singapore-138648

‡S hoklo Malaria Research Unit, Mae Sot, 68/30 Bantung Rd. Maesot TAK 63110 Thailand

Ψ Centre for Tropical Medicine, Nuffield Department of Clinical Medicine, Oxford University, Oxford, United Kingdom

† Department of Materials Science and Engineering, Massachusetts Institute of Technology, Cambridge-Massachusetts, 77 Massachusetts Avenue, MA 02139USA

$ Department of Biological Engineering, Massachusetts Institute of Technology, Cambridge-Massachusetts, 77 Massachusetts Ave. Cambridge, MA 02139 USA

* **Corresponding Authors: PRPreiser@ntu.edu.sg (P.R. Preiser) and mingdao@mit.edu (M. Dao)**

Footnotes

The authors acknowledge Singapore-MIT Alliance for Research & Technology (SMART) Centre funded by The National Research Foundation (NRF) for financial support. RC was partially supported by the start-up research grant (SRG LSC 2013 049) from Singapore University of Technology and Design (SUTD). MD and SS acknowledge partial support from the National Institutes of Health (NIH) Grant R01HL094270. Authors declare no conflict of interest.

A part of this research was presented at the following conferences

MAM 2012 Lorne- Australia: Molecular Approaches to Malaria, 19-23rd February.

ASTMH Meeting Washington DC: November 2013.

Corresponding Author: **Prof. Peter Rainer Preiser**
School of Biological Sciences
Nanyang Technological University
60 Nanyang Drive Singapore 637551
Republic of Singapore

Dr. Ming Dao
Department of Materials Science and Engineering, Massachusetts Institute of Technology, Cambridge-Massachusetts,
77 Massachusetts Avenue, MA 02139USA

Abstract (<150 words)

Malaria causes nearly 1 million deaths annually. Recent emergence of multi-drug resistance highlights the need to develop novel therapeutic interventions against human malaria. Given the involvement of sugar binding plasmodial proteins in host invasion, we set out to identify such proteins as targets of small glycans. Combining multi-disciplinary approaches, we report the discovery of a small molecule inhibitor, NIC capable of inhibiting host invasion through interacting with a major invasion-related protein, merozoite surface protein-1 (MSP-1). This interaction was validated through computational, biochemical and biophysical tools. Importantly, treatment with NIC prevented host invasion by *Plasmodium falciparum* and *Plasmodium vivax*- major causative organisms of human malaria. MSP-1, an indispensable antigen critical for invasion and suitably localized in abundance on the merozoite surface represents an ideal target for antimalarial development. The ability to target merozoite invasion proteins with specific small inhibitors opens up a new avenue to target this important pathogen.

Keywords: Malaria, *Plasmodium falciparum*, *Plasmodium vivax*, Glycan mimetic small molecules, Chemical Biology, Mass Spectrometry, Red Blood Cell, Host invasion, Merozoite Surface Proteins.

Text (Introduction> Methods> Results> Discussion: 3435 words)

Introduction

Malaria remains a major health concern for the developing world. Although recent trends suggest a progressive decline, nearly 220 million malaria infections (causing ~700,000 deaths) occurred in 2010 alone [1]. These data largely focus on *Plasmodium (P.) falciparum* infections in Africa and gravely underestimate the contribution of *Plasmodium vivax*, which may account for another 200 million infections in Asia and South America. Thus, malaria against which vaccine development efforts are still ongoing [2], exerts an enormous burden on global human health [3]. Efforts to treat malaria largely rely on chemotherapeutic approaches to block parasitic replication besides preventive measures targeting the mosquito vector. However, recent emergence of resistance against chloroquine [4] and reduced efficacy of artemisinin [5] point to the critical need for exploring new set of antimalarial targets.

Merozoite entry into erythrocytes is driven by complex recognition events between parasitic proteins and sugar moieties on the host red blood cells (RBCs) [6, 7]. Merozoites bind to sialic acid residues on RBC receptors for invasion [8], however, sialic acid-independent invasion pathways have also been elucidated [9, 10]. While several plasmodial proteins play critical roles during invasion, Merozoite Surface Proteins (MSPs) and Apical Membrane Antigens (AMAs) have been the most studied. Among MSPs, MSP-1 is considered a prime candidate for vaccine development [11, 12]. It is required for the attachment of merozoites to host receptors such as Band 3 [13] and for normal parasitic development [14]. MSP-1 undergoes two proteolytic processing steps during merozoite maturation [15]. Following cleavage, MSP-1 complex remains non-covalently attached to the merozoite surface until invasion, except for a small fragment of 19-kDa from the C-terminus (MSP-1_{19}) that remains attached to the merozoite even after invasion. Antibodies targeting MSP-1_{19} epitopes [16, 17] block merozoite invasion, illustrating a definite invasion-associated role of this domain. In addition, MSP-1_{19} is involved in normal parasitic development [17] and food vacuole formation [18].

Glycan derivatives interfere with replication and invasion of *P. falciparum* [19-21]. Especially, sulfated glycosaminoglycans are known to block merozoite [22] and sporozoite invasion [23]. It has been shown that heparin blocks merozoite invasion by binding to a specific domain of MSP-1 termed MSP-1_{33} thereby preventing the secondary proteolytic processing [24]. Although MSP-1_{19} does not bind to heparin-like glycosaminoglycan oligosaccharides [24], its ability to bind to small molecules has not been investigated. In this study, we report the identification of a small molecule, 2-butyl-5-chloro-3-(4-nitro-benzyl)-3H-imidazole-4-carbaldehyde (NIC) capable of binding to MSP-1_{19} of human malaria parasites: *P. falciparum* and *P. vivax*. Using different approaches, we demonstrate that NIC interacts with EGF-like domains present on MSP-1_{19}. These observations collectively point to the possibility of targeting plasmodial invasion proteins for antimalarial drug development.

Materials and Methods

Parasites and reagents

Collection of blood for Plasmodium culture was verified and approved by the Institutional Review Board (IRB) of National University of Singapore (NUS). *P. falciparum* strain, 3D7 was used for all experiments unless otherwise stated. Transgenic parasites - D10-*Pf*M3' and D10-*Pc*MEGF [34] were gifted by Paul Gilson and Danny Wilson (Burnet Institute, Australia). Various recombinant MSP-1_{19} (MRA 47, MRA 48, MRA 55 and MRA 60), antibodies (MRA 3, MRA 16) and parasites (Dd2, K1, T9-94, W2-mef and FCR3) were obtained from Malaria Research and Reference Reagent Resource Center (MR4). Parasites were synchronized by sorbitol selection or MACS- separation (Miltenyi Biotec). Parasitemia was scored by flow cytometric counting (LSRII flow cytometer- BD Biosciences) after staining with Hoechst. Dose-response curve generation and IC_{50} determination were performed with GraphPad Prism 5 using a four-parameter logistic curve (variable slope).

Virtual Screening and design of novel MSP-1 ligands

Insight II (Accelrys) was used for molecular modeling [42]. Automatic docking, clustering and energy minimizations [43] were performed using LigandFit module. A cavity detection algorithm and Monte Carlo conformational search algorithm were used for generating ligand poses consistent with active site shapes. Ligand poses at these sites were selected based on shape matching, using a cutoff distance of 3 Å. Structure based high-throughput virtual screening method of LigandFit (DS version 2.5) was used to identify potential ligands that interact with MSP-1 (PDB ID: X) using NCBI database [44]. Glycan-mimetic small molecules such as **KI-105**, **DMBO**, **BIC**, **NIC**, **CIC**, and **DIC** were

207 synthesized as reported [45]. These compounds were purified and characterized
208 using Agilent 1200 series LC system (Agilent ZORBAX, Eclipse-XDB-C18, 5
209 µm, 4.6 mm x 150 mm).

210 **Docking of small molecule ligands to MSP-1_{19}**

211 All ligands were subjected to LigandFit docking to determine reasonable
212 conformations for each low energy conformer at the binding site. Initially, crystal
213 structures of MSP-1_{19} from *P. falciparum* [25] (PDB ID: X), *P. vivax* [46] (PDB
214 ID: 2NPR) and *P. knowlesi* [47] (PDB ID: 1N1I) were used for docking. Further,
215 homology modeling of the MSP-1_{19} domains for *P. chabaudi*, *P. malariae* and *P.*
216 *ovale* were performed using 'build homology modeling' protocol by DS version
217 2.5.

218 **SPR measurements**

219 SPR measurements were conducted using a Biacore™ T-200 instrument
220 (Biacore, GE Healthcare). MSP-1_{19} peptide was directly immobilized onto a flow
221 cell on a CM5-S sensor chip (Biacore, GE Healthcare) through standard amine
222 coupling [48]. An empty flow cell was used as control. Surface was activated for
223 7 min with 1:1 mixture of 0.2 M N-ethyl-N'-[3-(diethylamino)propyl]carbodiimide
224 (EDC) and 0.05 M N-hydroxysuccinimde (NHS). Different interactants (in 10 mM
225 sodium acetate, pH 4.0) was injected across the activated surface at 10 µl/min
226 until desired immobilization level of ~3000 RU was achieved. The surface was
227 blocked with 7 min injection of 1 M ethanolamine-HCl, pH 8.5. Small molecules
228 were screened against the immobilized protein at a flow rate of 30 µl/min, with a
229 60-sec association phase and a 5-min dissociation phase, in running buffer (20
230 mM Na_2HPO_4-NaH_2PO_4, pH 7.4, 150 mM NaCl, 5% DMSO). Measurements for
231 affinity determination were performed under similar conditions using two fold

dilutions of 10 μM. Sensorgrams were double referenced [49] and evaluated with Scrubber 2 software. Equilibrium responses against concentration were fitted to a simple 1:1 binding isotherm using a global R_{max}. Each experiment was carried out at least 3 times. To validate the selectivity of binding and to approximately estimate the affinity constants, simulation exercise were carried out as reported [29].

Localization and affinity-enrichment of the target using NIC-Biotin

NIC**-** biotin was synthesized by amine coupling of the aldehyde group. Late-stage schizonts (~ 45 hpi) were treated with NIC-biotin for 4 h and aliquots were fixed (0.1 % paraformaldehyde/ PBS) and permeabilized (0.2 % Triton X100/PBS) in presence of Casein. After washing, samples were incubated with phycoerythrin-conjugated streptavidin (Invitrogen) and Hoechst for 30 min. Fluorescence microscopy was performed using an LSM 710 confocal microscope (Carl Zeiss). For affinity purifying NIC-reactive proteins, schizonts (~48 hpi) were fractionated into extra-parasitic and parasitic fractions by extraction with 0.02 % saponin and 1 % Triton X-100 sequentially. Samples were then diluted 1:5 with 20 mM sodium acetate buffer (pH 5.5), treated with 50 μM NIC-biotin for 2 h, and incubated with streptavidin-agarose beads (Thermo Scientific). After removing un-bound proteins by centrifugation, pellet was washed with PBS and proteins extracted for SDS-PAGE. Coomassie staining was carried out to visualize polypeptides. Protein bands were excised and subjected to MALDI/TOF-TOF analyses (4800 Proteomics Analyser- Applied Biosystems). MS data was searched using MASCOT v 2.1 (Matrix Science Ltd., London, UK) against NCBI Database. For examining target-specificity, affinity

enrichment experiments were performed with (1) non-biotinylated NIC, (2) in competition with excess of NIC (100 μM) and (3) denatured (SDS/heat) sample. Proteins bound to streptavidin beads were collected, resolved on SDS-PAGE for western blotting using anti-MSP-1 antibody.

***Plasmodium vivax ex vivo* invasion assays**

During February 2012, samples from *P. vivax* infected patients at Shoklo Malaria Research Unit (SMRU), Mae Sot region (Thailand) were collected after written informed consent. Cord blood was taken from three post healthy delivery placentas. The samples were collected as per ethical guidelines in the approved protocols: OXTREC 027-025 (University of Oxford, Centre for Clinical Vaccinology and Tropical Medicine, United Kingdom) and MUTM 2008-215 from the Ethics Committee of the Faculty of Tropical Medicine, Mahidol University, Bangkok. Leukocytes and platelets were removed using a CF11 column (Sriprawat et al., 2009) before conducting *P. vivax* invasion assays as previously described [36]**.** BCI (200 μM) and 25 μg/ml of anti-Duffy receptor DARC antibody (Gift by Drs Colin and Bertrand; Institut National de la Transfusion Sanguine, 75015 Paris, France) served as negative and positive controls respectively. To determine invasion rates, a 3 color cytometery method [37] using a field flow cytometer (BD Accuri® C6) was used. Flow cytometery data was verified with Giemsa-stained smears using microscopy.

Results

Identification of NIC as a potential ligand against EGF-like domains of Plasmodial MSP-1

Antibodies targeting EGF-like domains on the C-terminal motif (MSP-119) prevent host invasion. We therefore, set out to identify small molecules that can bind to MSP-1_{19} domain as invasion blockers. First, using the X-ray crystal structure of *P. falciparum* [25] a virtual screening was performed to prioritize small molecules that could interact with MSP-1_{19} of *P. falciparum.* Based on this screening, we chose KI-105 [26] and DMBO [27] that are known to interact with EGF-like domain containing proteins in other systems as promising ligands to interact with MSP-1_{19}. However, neither KI-105 nor DMBO exhibited any antimalarial activity against *P. falciparum*. Thus, we synthesized and evaluated other related scaffolds such as BIC, NIC, CIC, and DIC **(Supplemental Fig. S1A)** as binders of MSP-1_{19}. Among these, it was earlier demonstrated that NIC binds to vascular endothelial growth factor (VEGF) resulting in reduced cancer cell proliferation [28].

Based on these computational analyses, we posited that NIC could bind with a higher affinity to EGF-like domains present on MSP-1_{19} compared to other structurally related compounds **(Table. 1).** The energy-minimized structure of NIC is highlighted in **Fig.1A.** The ribbon diagram showing the structure of EGF-like domain of *Pf*MSP-1_{19} in complex with NIC is shown as a ball-and-stick model **(Fig.1B)**. Based on the structural complex of NIC with *Pf*MSP-1_{19}, the key residues positioned to make contact with NIC included Lys29, Cys30, Leu31, Leu32, Asn33, Tyr34, Lys35 and Gln36. NIC was likely to form additional bonds with Glu51, Asn52, Asn53, Gly54 and Gly55 **(Fig. 1C**). Also, it appears that NIC has the unique ability to bind to MSP-1_{19} through its ionic nitro-group on the benzene ring making it the most suitable ligand**.** Sequence alignment of residues within the EGF-like domains of MSP-1_{19} from multiple plasmodia revealed remarkable conservation of key residues that are positioned to make contact with NIC **(Fig. 1D).** Many of these conserved residues were within epitopes recognized by invasion-blocking antibodies against MSP-1.

NIC specifically interacts with *Pf*MSP-1_{19}

Computational analyses predicted that among KI-105 variants (BIC, NIC, CIC, and DIC), NIC had the highest binding affinity to MSP-1_{19}. This was validated via Surface Plasmon Resonance (SPR) measurements using recombinant *Pf*MSP-$1_{19,}$ where none of the small molecules showed detectable binding to *Pf*MSP-1_{19} except NIC **(Fig. 2A).** Notably, BCI, which served as the negative control as well as heparin, showed no measurable interaction with MSP-1_{19} as expected from previous reports [24].

We determined the affinity constant from a fit to a simple binding isotherm in an equilibrium analysis, with an estimated value in the tens of micromolar range (~ 37 μM) **(Fig. 2B).** Since we could not reach saturation of the surface due to lack of solubility of NIC at high concentrations (under conditions used for SPR measurements), and thus the calculated value of Rmax could not be precise, we chose to show the range for the value of affinity constant by simulating the Req values versus the NIC concentration for affinities of 25 μM and 50 μM and plotting the experimental values for Req at different concentrations of NIC, as adopted previously [29]. **Fig. 2B** shows that the values of responses for the measured interaction between NIC and *Pf*MSP-1_{19} do fall between 25 and 50 μM.

To validate the interaction of NIC with its parasitic target, we first conducted co-localization experiments using NIC-biotin **(Supplemental Fig. S1B**, **S1C**) that has comparable invasion inhibitory effects on malaria parasites as NIC **(Supplemental Fig. S1D)**. Using a parasite line that expresses MSP-1_{19}-GFP, we observed co-localization of NIC-biotin with MSP-1 in late-stage schizonts **(Fig. 2C).** In contrast, ring or trophozoite stage parasites when very little MSP-1 is present showed no detectable labeling with NIC-biotin **(Supplemental Fig. S1E).** However, due to the dispersed nature of GFP distribution in these parasites [30], it was not possible to conclusively document co-localization. Hence, fluorescence microscopy was repeated using antibodies against MSP-1_{19} together with NIC-biotin **(Supplemental Fig. S1 F)**; further supporting an interaction between NIC and MSP-1_{19}.

Next, we used NIC-biotin to identify parasitic targets. Schizont-stage parasites were fractionated into infected red cell/ extra-parasitic (iRBC) and parasitic fractions by differential extraction using saponin [31]. Further, each sample was incubated with 50 μM NIC-biotin and then with streptavidin- agarose beads to affinity purify proteins that interact with NIC. Aliquots from un-bound and bound fractions from each sample were resolved on SDS-PAGE and polypeptides visualized by Coomassie staining. Enrichment of a low molecular weight protein **(Fig. 2D)** was observed from the parasitic fraction and was identified as MSP-1_{19} through mass spectrometry **(Supplemental Fig. S1G)**. Importantly, no other proteins, including MSP-1_{33}- the target of heparin as reported previously [24] were enriched in the NIC-bound fraction. Specificity of NIC-biotin binding to MSP-1_{19} was confirmed by conditions such as (a) performing affinity-enrichment from parasitic extracts with NIC, (b) pre-treatment of the extract with 100 μM NIC prior to incubation with NIC-biotin and (c) by performing NIC-biotin incubation after denaturing the sample with SDS/heat **(Fig. 2E).** As expected, pre-treatment with excess NIC significantly reduced (30-50 %) the affinity enrichment of MSP-1_{19} by NIC-biotin. Due to the multiple steps involved in this experiment where each sample was processed individually, these results are primarily qualitative.

NIC blocks *P. falciparum* replication by impairing merozoite invasion

Assays were done on several *P. falciparum* strains to evaluate the effect of the small molecules on erythrocytic development. Trophozoite-stage parasites (~ 24 hpi) were allowed to grow until the next cycle in presence of inhibitors. DMSO and BCI served as negative controls. 48 h later, samples were collected, stained with Hoechst and parasitemia scored by flow cytometry. Amongst the scaffolds tested, only NIC inhibited parasite replication (**Fig. 3A**) with a median IC50 of 18 μM. Potential non-specific interaction of NIC with red cell proteins was ruled out by pre-incubating RBCs with NIC for 2 h and washing them prior to mixing with late-stage parasites. RBCs that were pre-treated with NIC supported normal parasite invasion and growth **(Fig. 3B).** Microscopic evaluation of Giemsa-stained smears revealed that NIC treatment resulted in impaired merozoite

invasion. Clumps of agglutinated merozoites were observed in smears prepared from post-rupture time points (**Fig. 3C**) after NIC treatment. NIC showed comparable inhibitory potential on a number of plasmodial strains tested **(Table. 2)** demonstrating a conserved target.

Further, ring stage parasites (~12 hpi) were treated with 20μM NIC and phenotypes monitored at specific intervals (15, 30, 45 and 60 hpi) using Giemsa-stained smears. By 60 hpi, all the schizonts had ruptured and established rings in the control (DMSO) vials while merozoites failed to invade in presence of NIC **(Fig. 3D).** The invasion inhibition by NIC was confirmed by live video microscopy [32]. In presence of NIC**,** the schizonts appeared to burst slowly and despite making initial contact with RBCs, merozoites failed to invade even after several minutes **(Supplemental Videos; S2A and S2B).** Next, invasion inhibition assays were conducted by mixing purified merozoites [33] with fresh RBCs in presence of NIC. This experiment revealed a strong and specific invasion inhibition in presence of NIC (**Fig. 3E).** Negative control (BCI) showed no significant inhibitory effects on invasion even at 200μM. Although there are minor differences in the sensitivity to the inhibitors of purified merozoites compared to intact schizonts, these experiments provide strong evidence for the invasion inhibitory activity of NIC. Furthermore, schizont-stage parasites (~ 45 hpi) were exposed for 2 h to NIC and NIC was removed by washing. These parasites were able to invade efficiently, revealing NIC's specific inhibitory effect solely on invasion **(Supplemental Fig. S1H).**

Computational docking revealed that NIC was likely to have superior binding affinity to MSP-1_{19} of *P. chabaudi* **(Supplemental: S3A**) compared to *Pf*MSP-1_{19}. Hence, we used a transgenic strain of *P. falciparum* (*Pc*MEGF) that has *Pc*MSP-1_{19} swapped in [34] to evaluate its sensitivity to NIC. Dose-dependent effect of NIC on replication of *Pc*MEGF was examined together with the control parasites (*Pf*M3') that contain the original *Pf*MSP-1_{19}. This revealed significantly higher sensitivity of the *Pc*MEGF parasites to NIC **(Fig. 3F)** compared to *Pf*M3'**,** in agreement with the computational predictions. BCI-treated parasites (*Pf*M3' and *Pc*MEGF) served as controls and showed no apparent differences in

sensitivity **(Fig. 3G).** These data functionally validate the interaction between NIC and MSP-1_{19}, leading to impairment of invasion.

NIC inhibits *P. vivax* invasion

The residues within EGF-like domains of MSP-1_{19}, are significantly conserved amongst multiple plasmodia. Computational analyses predicted that MSP-1_{19} from several human malaria parasites were likely to bind to NIC **(Supplemental: S3B).** Hence, we inspected the interaction of NIC with *Pv*MSP-1_{19}, EGF-like domains of which are critical for reticulocyte invasion [35] by *P. vivax*. SPR measurements using recombinant *Pv*MSP-1_{19} confirmed specific interaction of NIC with the target **(Fig. 4A),** however with lower affinity compared to *Pf*MSP-1_{19} **(Fig. 4B).** The effect of NIC on *ex vivo* invasion of *P. vivax* into human reticulocytes was tested using a recently developed assay [36]. Purified schizonts from clinical isolates were mixed with enriched reticulocytes in presence of different amounts of NIC. BCI-treated parasites served as negative control while an anti- Duffy antibody (2C3) that blocks invasion at 25 μg/ml concentration served as positive control. After 24 hours, newly invaded reticulocytes were counted by a field-based flow cytometry assay [37] (**Fig. 4C**). A concentration-dependent inhibition of invasion by NIC on *P. vivax* merozoites was observed with an average IC 50 of 23.6 μM. BCI showed no inhibition even at 100 μM concentration. These results were further verified by microscopic inspection of Giemsa-stained blood smears **(Fig. 4D).** In BCI-treated samples, robust invasion was observed **(Fig. 4D- Upper Panel)** while very few ring-stage infections were found in samples that were incubated with 25 μM or 100 μM NIC **(Fig. 4D- Middle and Lower Panels).** Finally, six independent analyses were carried out using different field isolates - all of them demonstrated dose-dependent inhibition of invasion caused by NIC (**Fig. 4E**), with a Median IC50 of 23.6μM (IQR 16.9-27.24). These observations are consistent with other results and strongly support the idea that NIC has broad affinity to MSP1_{19} from multiple forms of human malaria.

Discussion

Host invasion by plasmodia is facilitated by coordinated action of merozoite surface proteins [38], proteases [39, 40] and signaling molecules such as calcium [41]. Extra-cellular merozoites have a short life span; they become nonviable within minutes of release making strategies targeting invasion an attractive proposition. Prior research explored invasion-related proteases [39, 40] as well as antibodies for potential therapeutic development. However, the likely off-target effects of protease inhibitors and permeability limitations of antibodies hinder these approaches significantly.

Chemical biology tools allow detailed and targeted investigation of complex biological events, such as malaria parasite invasion. MSP-1 is the most abundant invasion protein and binds to glycan residues on RBC to initiate host entry. The smaller fragment derived from MSP-1 processing; MSP-1_{19} is critical for invasion and parasite development. It shows less polymorphism (within it's EGF-like domains) highlighting suitability as a pan-plasmodial target. We conducted *in silico* and *in vitro* screening to identify a small molecule, NIC with significant binding affinity to both recombinant and parasitic *Pf*MSP-1_{19} that inhibits merozoite invasion. While at this stage we do not fully understand the detailed molecular mechanism leading to invasion inhibition by NIC binding to MSP-1, our results represent a major advancement in the hunt for anti-malarials with pan-species efficacy. NIC was able to bind to MSP-1 and inhibit invasion not only upon merozoite release, but also within late-stage schizonts. This highlights the permeability advantages of small molecules over therapeutic

antibodies. Efforts to optimize molecular structures from the NIC lineage with stronger/irreversible binding properties to MSP-1 may provide a platform to further consider these molecules for *in vivo* experiments and detailed pharmacological profiling.

The abundance, accessible cellular localization and indispensable nature of invasion proteins make them promising drug targets. In the Plasmodial genome, there are several proteins with putative EGF-like domains. Other members of the MSP family, MSP4 and MSP8 as well as lesser-known proteins such as PF3D7-1403200 and PF3D7-1002300 (www.plasmodb.org) contain such domains. It would be desirable to study these proteins/domains as candidate targets to design small molecule scaffolds; individually or as a 'group target'. Designing small molecules to target invasion proteins offer a viable option in the development of a resistance-free drug against human malaria.

References

1. http://www.who.int/malaria/world_malaria_report_2011/en/.
2. Agnandji ST *et al.* (2011) First results of phase 3 trial of RTS,S/AS01.malaria vaccine in African children. *N Engl J Med*. **365** (20),1863-75.
3. Murray CJ, Rosenfeld LC, Lim SS, Andrews KG, Foreman KJ, Haring D, Fullman N, Naghavi M, Lozano R, Lopez AD (2012) Global malaria mortality between 1980 and 2010: a systematic analysis. *Lancet*. **379** (9814): 413-31. doi: 10.1016/S0140-6736 (12) 60034-8.
4. Mita T, Tanabe K, Kita K (2009) Spread and evolution of *Plasmodium falciparum* drug resistance. *Parasitol. Int*. **58** (3), 201-9.
5. O'Brien C, Henrich PP, Passi N, Fidock DA (2011) Recent clinical and molecular insights into emerging artemisinin resistance in *Plasmodium falciparum*. *Curr Opin Infect Dis*. **24** (6), 570-7.
6. Breuer WV, Kahane I, Baruch D, Ginsburg H, Cabantchik ZI (1983). Role of internal domains of glycophorin in *Plasmodium falciparum* invasion of human erythrocytes. *Infect Immun*. **42** (1): 133-40.
7. Mayer DC, Cofie J, Jiang L, Hartl DL, Tracy E, Kabat J, Mendoza LH, Miller LH (2009) Glycophorin B is the erythrocyte receptor of *Plasmodium falciparum* erythrocyte-binding ligand, EBL-1. *Proc Natl Acad Sci U S A*. **106** (13), 5348-52.

8. Sim BK, Chitnis CE, Wasniowska K, Hadley TJ, Miller LH (1994) Receptor and ligand domains for invasion of erythrocytes by *Plasmodium falciparum*. Science. ***264*** (5167), 1941-4.

9. Duraisingh MT, Maier AG, Triglia T, Cowman AF (2003) Erythrocyte- binding antigen 175 mediates invasion in *Plasmodium falciparum* utilizing sialic acid-dependent and independent pathways. *Proc. Natl. Acad. Sci. U S A.* **100** (8), 4796- 801.

10. Spadafora C, Awandare GA, Kopydlowski KM, Czege J, Moch JK, Finberg RW, Tsokos GC, Stoute JA (2010) Complement receptor 1 is a sialic acid-independent erythrocyte receptor of *Plasmodium falciparum*. *PLoS Pathog*. **6** (6), e1000968.

11. Langermans JA, Hensmann M, van Gijlswiik M, Zhang D, Pan W, Giersing BK, Locke E, Dubovsk F, Wittes J, Thomas AW (2006) Preclinical evaluation of a chimeric malaria vaccine candidate in Montanide ISA 720: immunogenicity and safety in rhesus macaques. *Hum Vaccin*. **2** (5), 222- 6.

12. Ellis RD *et al*. (2010) Phase 1 trial of the *Plasmodium falciparum* blood stage vaccine MSP1 (42)- C1/Alhydrogel with and without CPG 7909 in malaria naïve adults. *PLoS One*. **5** (1), e8787.

13. Goel VK, Li X, Chen H, Liu SC, Chishti AH, Oh SS (2003) Band 3 is a host receptor binding merozoite surface protein 1 during the *Plasmodium falciparum* invasion of erythrocytes. *Proc. Natl. Acad. Sci. U S A*. **100** (9), 5164- 9.

14. Child MA, Epp C, Bujard H, Blackman MJ (2010) Regulated maturation of malaria merozoite surface protein-1 is essential for parasite growth. *Mol Microbiol.* **78** (1), 187- 202.

15. Holder AA, Blackman MJ, Burghaus PA, Chappel JA, Ling IT, McCallum-Deighton N, Shai S (1992) A malaria merozoite surface protein (MSP1)-structure, processing and function. *Mem Inst Oswaldo Cruz*. 87 Suppl ***3***: 37-42.

16. Chappel JA, Holder, A.A. (1993) Monoclonal antibodies that inhibit Plasmodium falciparum invasion in vitro recognise the first growth factor- like domain of merozoite surface protein-1. *Mol Biochem Parasitol*. **60** (2),303- 11.

17. Moss DK, Remarque EJ, Faber BW, Cavanagh DR, Arnot DE, Thomas AW, Holder AA (2012) *Plasmodium falciparum* 19-kilodalton merozoite surface protein 1 (MSP1)-specific antibodies that interfere with parasite growth in vitro can inhibit MSP1 processing, merozoite invasion, and intracellular parasite development. *Infect Immun.* ***80*** (3): 1280-7.

18. Dluzewski AR, Ling IT, Hopkins JM, Grainger M, Margos G, Mitchell GH, Holder AA, Bannister LH (2008) Formation of the food vacuole in *Plasmodium falciparum*: a potential role for the 19kDa fragment of merozoite surface protein 1 (MSP1(19)). *PLoS One*. **3** (8), e3085.

19. Xiao L, Yang C, Patterson PS, Udhayakumar V, Lal AA (1996)

574 Sulfated polyanions inhibit invasion of erythrocytes by plasmodial
575 merozoites and cytoadherence of endothelial cells to parasitized
576 erythrocytes. *Infect Immun*. **64** (4), 1373- 8.
577 20. Kisilevsky R, Crandall I, Szarek WA, Bhat S, Tan C, Boudreau L,
578 Kain KC (2002) Short-chain aliphatic polysulfonates inhibit the
579 entry of Plasmodium into red blood cells. *Antimicrob Agents*
580 *Chemother.* **46** (8), 2619- 26.
581 21. Adams Y, Freeman C, Schwartz-Albiez R, Ferro V, Parish CR,
582 Andrews KT (2006) Inhibition of *Plasmodium falciparum* growth in
583 vitro and adhesion to chondroitin-4-sulfate by the heparan
584 sulfate mimetic PI-88 and other sulfated oligosaccharides.
585 *Antimicrob Agents Chemother* **50** (8), 2850- 2.
586 22. Dalton JP, Hudson D, Adams JH, Miller LH (1991) Blocking of
587 the receptor-mediated invasion of erythrocytes by *Plasmodium*
588 *knowlesi* malaria with sulfated polysaccharides and
589 glycosaminoglycans. *Eur J Biochem*. **195** (3), 789- 94.
590 23. Basseri HR, Doosti S, Akbarzadeh K, Nateghpour M, Whitten MM,
591 Ladoni H (2008) Competency of Anopheles stephensimysorensis
592 strain for *Plasmodium vivax* and the role of inhibitory
593 carbohydrates to block its sporogenic cycle. *Malar J*. **7**, 131.
594 24. Boyle MJ, Richards JS, Gilson PR, Chai W, Beeson JG (2010)
595 Interactions with heparin-like molecules during erythrocyte
596 invasion by *Plasmodium falciparum* merozoites. *Blood*. **115** (22),
597 4559- 68.

598 25. Morgan WD, Birdsall B, Frenkiel TA, Gradwell MG, Burghaus
599 PA, Syed SE, Uthaipibull C, Holder AA, Feeney J (1999) Solution
600 structure of an EGF module pair from the Plasmodium falciparum
601 merozoite surface protein 1. *J Mol Biol*. **289** (1), 113-22.
602 26. Ishida K, Wierzba MK, Teruya T, Simizu S, Osada H (2004)
603 Novel heparansulfate mimetic compounds as antitumor agents.
604 *Chem Biol*. **11** (3), 367- 77.
605 27. Basappa, Murugan S, Kavitha CV, Purushothaman A, Nevin KG,
606 Sugahara K, Rangappa KS (2010) A small oxazine compound as
607 an anti-tumor agent: a novel pyranoside mimetic that binds to
608 VEGF, HB- EGF, and TNF-α. *Cancer Lett* **297,** (2), 231- 43.
609 28. Basappa, Sugahara K, Thimmaiah KN, Bid HK, Houghton PJ,
610 Rangappa KS (2012) Anti-tumor activity of a novel HS-mimetic
611 vascular endothelial growth factor Binding small molecule. *PLoS*
612 *ONE* **7** (8): e39444. doi: 10.1371/journal.pone.0039444.
613 29. Wei L, Jiang P, Yau YH, Summer H, Shochat SG, Mu Y,
614 Pervushin K (2009) Residual structure in islet amyloid polypeptide
615 mediates its interactions with soluble insulin. Biochemistry. 48 (11):
616 2368-76.
617 30. Wilson DW, Crabb BS, Beeson JG (2010) Development of
618 fluorescent *Plasmodium falciparum* for *in vitro* growth inhibition
619 assays. *Malar J*. **9,**152.
620 31. Chandramohanadas R, Davis PH, Beiting DP, Harbut MB, Darling
621 C, Velmourougane G, Lee MY, Greer PA, Roos DS, Greenbaum
622 DC.(2009) Apicomplexan parasites co-opt host calpains to

facilitate their escape from infected cells. *Science*. **324**(5928), 794-7.

32. Treeck M, Zacherl S, Herrmann S, Cabrera A, Kono M, Struck NS, Engelberg K, Haase S, Frischknecht F, Miura K *et al.* (2009) Functional analysis of the leading malaria vaccine candidate AMA-1 reveals an essential role for the cytoplasmic domain in the invasion process. *PLoS Pathog*. **5** (3), e1000322 (2009).

33. Boyle MJ, Wilson DW, Richards JS, Riglar DT, Tetteh KK, Conway DJ, Ralph SA, Baum J, Beeson JG (2010) Isolation of viable *Plasmodium falciparum* merozoites to define erythrocyte invasion events and advance vaccine and drug development. *Proc Natl Acad Sci U S A*, **107**(32), 14378- 83.

34. O'Donnell RA, de Koning-Ward TF, Burt RA, Bockarie M, Reeder JC, Cowman AF, Crabb BS (2001) Antibodies against merozoite surface protein (MSP)-1(19) are a major component of the invasion-inhibitory response in individuals immune to malaria. *J Exp Med*. **193** (12), 1403- 12.

35. Han HJ, Park SG, Kim SH, Hwang SY, Han J, Traicoff J, Kho WG, Chung JY (2004) Epidermal growth factor-like motifs 1 and 2 of *Plasmodium vivax* merozoite surface protein 1 are critical domains in erythrocyte invasion. *Biochem Biophys Res Commun*. **320** (2), 563-70.

36. Russell B, Suwanarusk R, Borlon C, Costa FT, Chu CS, Rijken MJ, Sriprawat K, Warter L, Koh EG, Malleret B *et al.* (2011) A

reliable *ex vivo* invasion assay of human reticulocytes by *Plasmodium vivax*. *Blood*. **118** (13), e74-81 (2011).

37. Malleret B, Claser C, Ong AS, Suwanarusk R, Sriprawat K, Howland SW, Russell B, Nosten F, Rénia L (2011) A rapid and robust tri-color flow cytometry assay for monitoring malaria parasite development. *Sci Rep*. **1**, 118.

38. Iyer J, Grüner AC, Rénia L, Snounou G, Preiser PR (2007) Invasion of host cells by malaria parasites: a tale of two protein families. *Mol Microbiol*. **65** (2), 231-49.

39. Greenbaum DC, Baruch A, Grainger M, Bozdech Z, Medzihradszky KF, Engel J, DeRisi J, Holder AA, Bogyo M (2002) A role for the protease falcipain 1 in host cell invasion by the human malaria parasite. *Science*. **298** (5600), 2002- 6.

40. Koussis K, Withers-Martinez C, Yeoh S, Child M, Hackett F, Knuepfer E, Juliano L, Woehlbier U, Bujard H, Blackman MJ (2009) A multifunctional serine protease primes the malaria parasite for red blood cell invasion. *EMBO J*. **28** (6), 725- 35.

41. Singh S, Alam MM, Pal-Bhowmick I, Brzostowski JA, Chitnis CE (2010) Distinct external signals trigger sequential release of apical organelles during erythrocyte invasion by malaria parasites. *PLoS Pathog*. **6** (2), e1000746.

42. Wu G, Robertson DH, Brooks CL 3rd, Vieth M (2003) Detailed analysis of grid-based molecular docking: A case study of CDOCKER- A CHARMm-based MD docking algorithm. *J Comput Chem*. **24** (13), 1549- 62.

672 43. Venkatachalam CM, Jiang X, Oldfield T, Waldman M (2003)
673 LigandFit: a novel method for the shape-directed rapid docking
674 of ligands to protein active sites. *J Mol Graph Model*. **21**(4), 289-
675 307.
676 44. Shoichet BK (2004) Virtual screening of chemical libraries. *Nature*.
677 **432** (7019), 862- 5.
678 45. Gaonkar SL, Lokanatha Rai KM, Suchetha Shetty N (2009)
679 Microwave- assisted synthesis and evaluation of anti-
680 inflammatory activity of new series of N- substituted 2-butyl-5-
681 chloro- 3 H-imidazole- 4- carbaldehyde derivatives. *Medicinal*
682 *Chemistry Research*. **18**, (3), 221- 230.
683 46. Babon JJ, Morgan WD, Kelly G, Eccleston JF, Feeney J, Holder
684 AA (2007) Structural studies on *Plasmodium vivax* merozoite
685 surface protein-1. *Mol Biochem Parasitol* **153** (1), 31- 40.
686 47. Garman SC, Simcoke WN, Stowers AW, Garboczi DN (2003)
687 Structure of the C-terminal domains of merozoite surface protein-1
688 from *Plasmodium knowlesi* reveals a novel histidine binding site. *J*
689 *Biol Chem*. **278** (9), 7264-9.
690 48. Johnsson B, Löfås S, Lindquist G (1991) Immobilization of proteins
691 to a carboxymethyldextran-modified gold surface for biospecific
692 interaction analysis in surface plasmon resonance sensors.
693 *Analytical Biochemistry*. **198** (2), 268-277.
694 49. Myszka DG (1999) Improving biosensor analysis. *J. Mol. Recognit.*
695 **12** (5), 279- 84.

50. Sriprawat K, Kaewpongsri S, Suwanarusk R, Leimanis ML, Lek-Uthai U, Phyo AP, Snounou G, Russell B, Renia L, Nosten F (2009) Effective and cheap removal of leukocytes and platelets from *Plasmodium vivax* infected blood. *Malar. J*. **8**, 115.

Acknowledgements

We thank MR4 for various recombinant proteins and antibodies and Brendon Crabb, Paul Gilson and Dany Wilson for providing transgenic parasites (D10-*Pf*M3 and D10-*Pc*MEGF). The support from the core facility at the Department of Biological Sciences- NUS in performing Mass Spectrometry Analysis is thankfully acknowledged.

Conflict of Interest

The authors declare that they have no conflict of interest.

Author Contributions:

RC: Designed, performed and coordinated research, analyzed the data and wrote the manuscript **BB:** Provided reagents, performed computational analyses and assisted in manuscript preparation **BR**: Involved in *P. vivax* study design, Performed *P. vivax* invasion assays, analyzed the data, verified results and assisted in manuscript preparation **KL:** Performed *P. falciparum* experiments and assisted in manuscript preparation **YH**: Performed SPR analyses **LM**: Assisted with *P. falciparum* experiments **AC**: Assisted with *P. falciparum* experiments **KG**: Performed microscopy analysis **LR:** Involved in *P. vivax* study design and verified results **FN:** Provided reagents and other tools for research, contributed to ethical clearance **SGS**: Involved in SPR study design, provided research tools and verified SPR results **RS:** Involved in study design**,** provided tools for Research & verified results **MD**: Involved in study design, provided tools for Research & verified results **SS**: Involved in study design, provided tools for Research & verified the results **PRP**: Contributed to study design, Provided tools for Research & verified the results and wrote the manuscript.

747 **Figure legends**

748

749 **Fig. 1: Prediction of NIC as a small molecule scaffold with potential**
750 **binding affinity to MSP-1_{19} of *P. falciparum* (A)** energy minimized structure of
751 NIC highlighting its ionic functional groups (highlighted with arrowheads) is
752 shown **(B)** Ribbon diagram of the structure of EGF-like domain of *Pf*MSP-1_{19} in
753 complex with NIC is shown. Secondary structure of the protein is shown with α-
754 helices and β-strands, while NIC is represented in ball-and-stick model (green
755 for carbon, blue for oxygen, white for hydrogen, and yellow for sulphur) **(C)**
756 Interaction map showing the key amino acids at *Pf*MSP-1_{19} that are positioned
757 to make interactions with NIC. The hydrogen bonding is shown in red **(D)**
758 Sequence alignment of C-terminal residues of MSP-1_{19} of various plasmodial
759 species: conserved amino acid residues are in blue, residues that are likely to
760 interact with NIC are highlighted in Red.

761

762 **Fig. 2: NIC interacts specifically with MSP-1_{19} of *P. falciparum* (A)** SPR
763 Interaction analysis of NIC over immobilized *Pf*MSP-1_{19}. Immobilization was
764 performed by amine coupling to a CM5 sensor chip to the level of 3000 RU. NIC
765 (concentrations) was injected sequentially over the relevant and control
766 surfaces. The sensorgrams were fit using the steady state affinity model from
767 Scrubber software. Each experiment was carried out at least 3 times to confirm
768 the results **(B)** Experimental values of Req for the corrected sensorgrams were
769 compared to the simulated values for K_D=10 μM and 50 μM. The value for the
770 affinity constant cannot be determined from equilibrium analysis (see results)
771 and was estimated to be between these two values (37 μM as calculated from

772 the fit). **(C)** Fluorescent microscopy analyses using NIC-biotin reveals the target
773 on merozoite surface, co-localizing with MSP-1_{19}-GFP **(D)** Affinity purification of
774 proteins using 50 μM NIC-biotin shows specific enrichment of MSP-1_{19}. Magnet
775 purified parasites were fractionated into extra-parasitic and merozoite fractions
776 and incubated with NIC-biotin. SDS-PAGE analysis of biotinylated proteins
777 showed specific enrichment of a polypeptide later confirmed to be MSP-1_{19} by
778 mass spectrometry analysis and western blot. **(E)** Affinity pull-out experiments of
779 parasitic material using 50μM NIC-biotin (Lane A), 50μM NIC (Lane B), 100μM
780 NIC followed by 50μM NIC-biotin (Lane C) and under denaturing conditions
781 (Lane D). The latter 3 conditions significantly reduced the extent of *Pf*MSP-1_{19}
782 enrichment.
783
784 **Fig. 3: Evaluation of invasion-blocking properties of NIC in *P. falciparum***
785 **(A)** Dose-dependent effect of 4 major small molecule scaffolds on the replication
786 of *P. falciparum*; NIC shows a significant and specific inhibition of parasite
787 replication (transition from schizonts to ring) with an average IC50 of 18 μM,
788 error bars show standard deviation, the figure represents compiled data from 3
789 independent experiments (B) RBCs pre-incubated with NIC and washed prior to
790 parasite infection, supports normal invasion and growth ruling out non-specific
791 binding of NIC to red cell proteins **(C)** Microscopic analysis of representative
792 Giemsa-stained smears from inhibitor-treated parasites (DMSO, BCI, BIC, NIC,
793 DIC and CIC each at 25 μM) demonstrate that treatment with NIC resulted in an
794 invasion defective phenotype, clumps of extra-cellular merozoites that were
795 unable to invade was observed. None of the other inhibitors induced similar
796 phenotypes at the tested concentration **(D)** Stage-specific effect of NIC (25μM)

on *P. falciparum* development demonstrating a specific inhibitory effect on invasion **(E)** The inhibitory effect of NIC on red cell invasion by purified merozoites, the figure shows combined data from 4 independent experiments and error bars indicate standard deviation **(F)** Transgenic parasites (*Pc*MEGF) that contain MSP-1_{19} from *Plasmodium chabaudi* (*Pc*MSP-1_{19}) at schizont stages were allowed to rupture and invade in presence of NIC**.** These parasites showed increased sensitivity to NIC compared to wild-type (*Pf*M3') parasites. The figure represent combined results from 3 independent experiments, error bars show standard deviation. **(G)** Transgenic parasites (*Pc*MEGF) that contain MSP-1_{19} from *Plasmodium chabaudi* (*Pc*MSP-1_{19}) when allowed to rupture and invade in presence of BCI, showed no differences in their sensitivity. The figure represent combined results from 3 independent experiments, error bars show standard deviation.

Fig. 4: NIC binds to *Pv*MSP-1_{19} and shows anti-invasive activity against clinical isolates of *P. vivax* (A) SPR measurements using recombinant *Pv*MSP-1_{19} reveal specific binding of NIC with the target antigen. Immobilization, the binding assay and the determination of the affinity were performed as in Fig 2. **(B)** Experimental values of Req for the corrected sensorgrams were compared to the simulated values for K_D=10 µM and 50 µM. The value for the affinity constant cannot be determined from equilibrium analysis (see results) and was estimated to be between these two values. **(C)** An *ex vivo* assay on six Thai Isolates of *P. vivax* showed that NIC had a dose dependent inhibitory effect on the invasion of human cord reticulocytes by *P. vivax*, as determined by flow cytometry; BCI as well as an antibody against Duffy protein served as negative

and positive controls respectively **(D)** Microscopic analyses of the Giemsa-stained smears collected from inhibitor-treated cultures reveal blockage of invasion by *P. vivax* in presence of NIC **(E)** Compiled data derived from the treatment with NIC of six Thai *P. vivax* isolates analyzed using a nonlinear sigmiodal model provide a median IC50 of 23.6 μM.

Table: 1: Summary of docking and scoring analyses amongst the selected small molecule scaffolds against *Pf*MSP-1_{19}. (Abbreviations: **PLP1**: Piecewise Linear Potential 1, **PLP2**: Piecewise Linear Potential 2, **LigScore1 & 2**: (fast, simple, scoring function for predicting receptor-ligand binding affinities) **Jain**: empirical scoring function through an evaluation of the structures and binding affinities of a series of protein-ligand complexes, **PMF**: Potential of Mean Force, **LIE**: ligand internal energy, **DS**: Dock Score).

Table. 2: Effect of NIC on various strains of *P. falciparum*, based on replication assays (using schizont-stage parasites). The values represent compiled results from 3 independent experiments.

847 **Supplemental Material**

848

849 **S1: (A)** Chemical structures of all the small molecules that were designed and
850 tested as MSP-1_{19} ligands as part of this study are provided **(B)** Separation and
851 isolation of NIC-biotin (MW: 599.18) using HPLC **(C)** Molecular structure of NIC-
852 biotin synthesized through amine coupling of biotin to NIC **(D)** Comparison of
853 invasion inhibitory activity of NIC and NIC-biotin on parasite invasion **(E)** Labeling
854 and visualization of ring and trophozoite stage *P. falciparum* using NIC-biotin,
855 early stage parasites show no detectable labeling with NIC-biotin, in agreement
856 with low levels of MSP-1 expression during early stages of parasite development
857 **(F)** Co-localization of MSP-1 (using an antibody) and NIC-biotin using
858 immunofluorescence microscopy **(G)** Mass spectrometric identification of MSP-
859 1_{19} fragments through affinity enrichment using NIC-biotin. NIC-biotin pulled out
860 MSP-1_{19} from parasitic fraction while the iRBC fraction showed non-specific
861 enrichment of red cell globin. **(H)** Schizont-stage parasites incubated with NIC
862 followed by NIC removal prior to egress/ invasion shows no significant inhibition
863 of invasion.

864

865 **S2: (A)** Live video (Representative) of *P. falciparum* schizonts during rupture
866 after treatment with BCI. Most merozoites from such treatments were released
867 and invaded fresh RBCs within 2 minutes. **(B)** Live video (Representative) of *P.*
868 *falciparum* schizonts during rupture after treatment with NIC. Treatment with NIC
869 slowed down schizont bursting and the released merozoites failed to invade even
870 after several minutes and eventually became no viable.

871

872 **S3: (A) Summary of docking and scoring analyses of NIC against *Pc*MSP-**
873 **1_{19} in comparison to *Pf*MSP-1_{19}.** Docking exercise revealed significantly higher
874 binding affinity of *Pc*MSP-1_{19} to NIC compared to *Pf*MSP-$1_{19.}$ (**B) Summary of**
875 **docking analyses between NIC and MSP-1_{19} of various malarial species**
876 **that infect humans**. This exercise demonstrated that NIC has comparable
877 affinities to the target antigen of all species.
878

Fig. 1

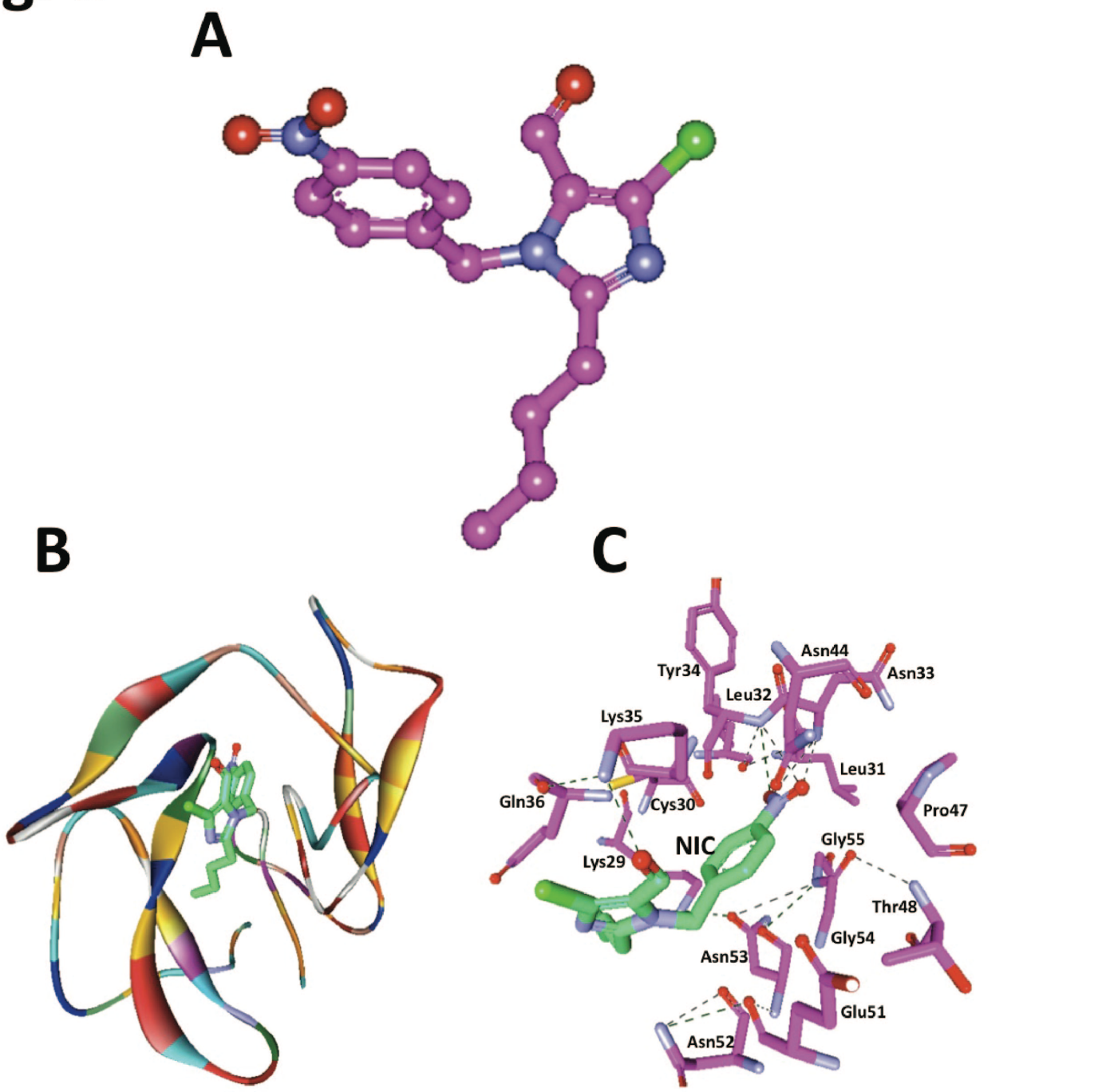
A
B
C
Tyr34
Asn44
Asn33
Leu32
Lys35
Leu31
Gln36
Cys30
Pro47
NIC
Gly55
Lys29
Thr48
Gly54
Asn53
Glu51
Asn52

D

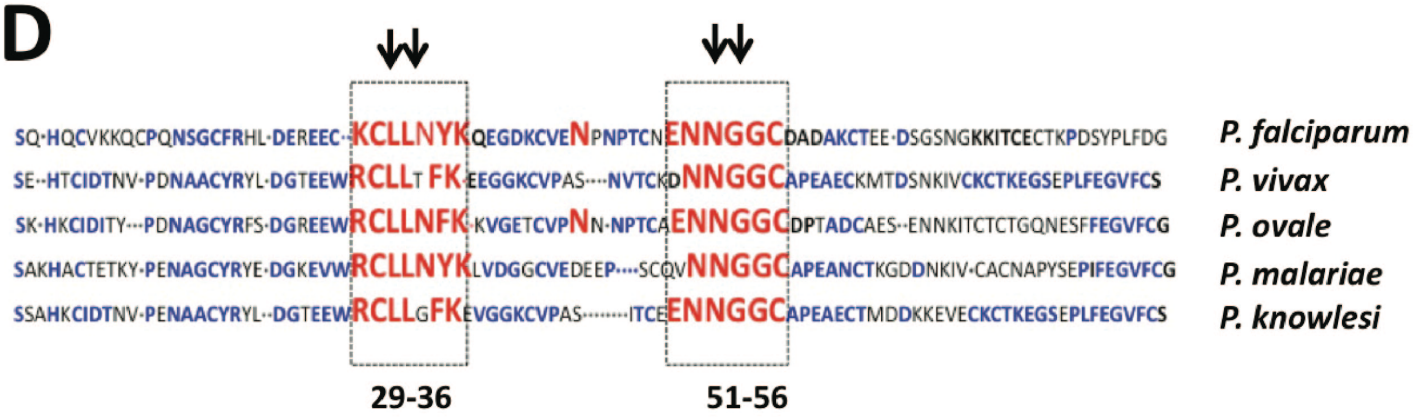
SQ·HQCVKKQCPQNSGCFRHL·DEREEC··KCLLNYKQEGDKCVENPNPTCNENNGGCDADAKCTEE·DSGSNGKKITCECTKPDSYPLFDG
SE··HTCIDTNV·PDNAACYRYL·DGTEEWRCLLT FK·EEGGKCVPAS····NVTCKDNNGGCAPEAECKMTDSNKIVCKCTKEGSEPLFEGVFCS
SK·HKCIDITY···PDNAGCYRFS·DGREEWRCLLNFK·KVGETCVPNN·NPTCAENNGGCDPTADCAES··ENNKITCTCTGQNESFFEGVFCG
SAKHACTETKY·PENAGCYRYE·DGKEVWRCLLNYKLVDGGCVEDEEP····SCQVNNGGCAPEANCTKGDDNKIV·CACNAPYSEPIFEGVFCG
SSAHKCIDTNV·PENAACYRYL··DGTEEWRCLLGFKEVGGKCVPAS·····ITCEENNGGCAPEAECTMDDKKEVECKCTKEGSEPLFEGVFCS
P. falciparum
P. vivax
P. ovale
P. malariae
P. knowlesi
29-36
51-56

Fig. 2

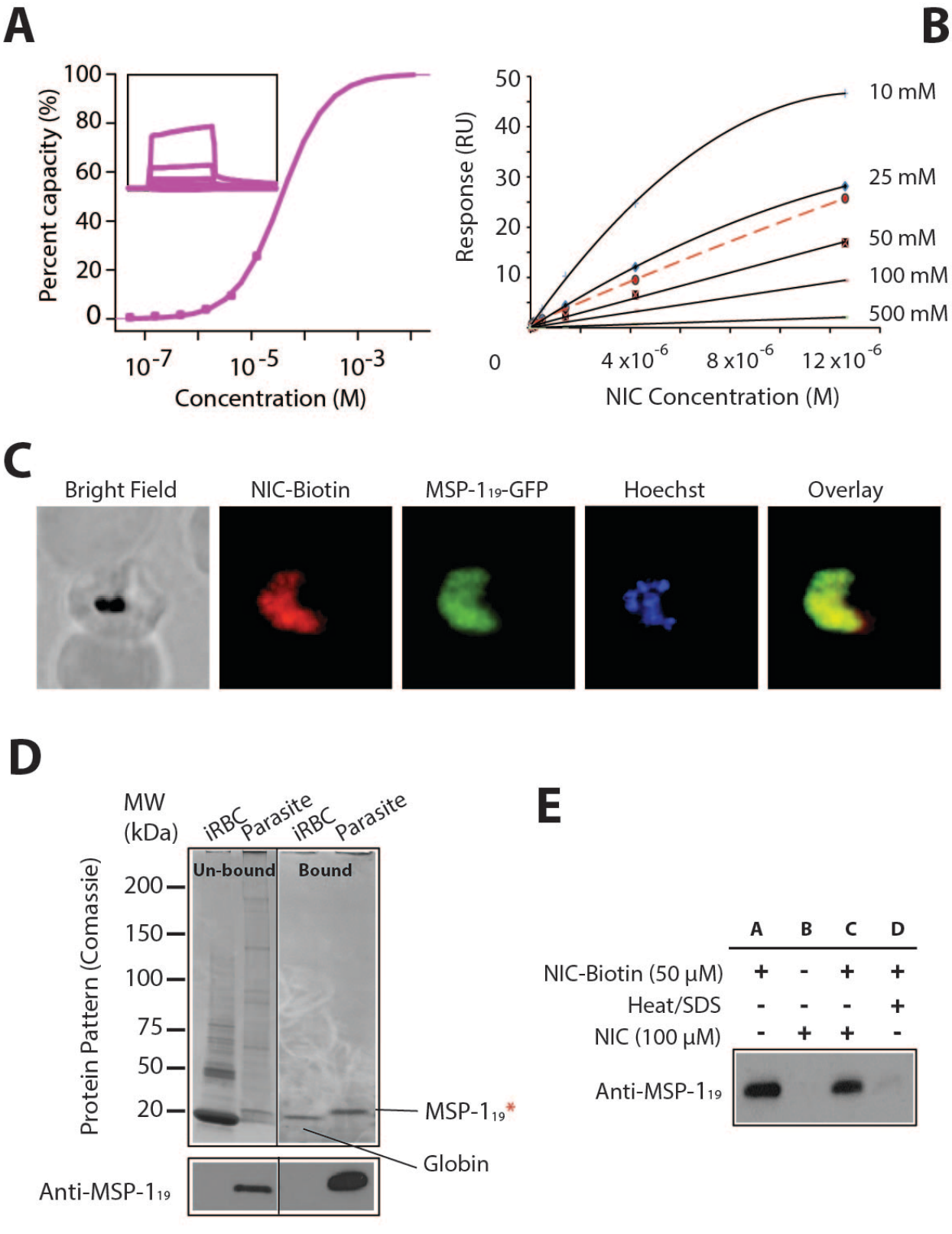
A
B
Percent capacity (%)
100
80
60
40
20
0
10^{-7}
10^{-5}
10^{-3}
Concentration (M)
Response (RU)
50
40
30
20
10
0
10 mM
25 mM
50 mM
100 mM
500 mM
4×10^{-6}
8×10^{-6}
12×10^{-6}
NIC Concentration (M)
C
Bright Field
NIC-Biotin
MSP-1_{19}-GFP
Hoechst
Overlay
D
MW (kDa)
iRBC
Parasite
iRBC
Parasite
Un-bound
Bound
Protein Pattern (Comassie)
200
150
100
75
50
20
MSP-1_{19}*
Globin
Anti-MSP-1_{19}
E
A
B
C
D
NIC-Biotin (50 µM) + - + +
Heat/SDS - - - +
NIC (100 µM) - + + -
Anti-MSP-1_{19}

Fig. 3

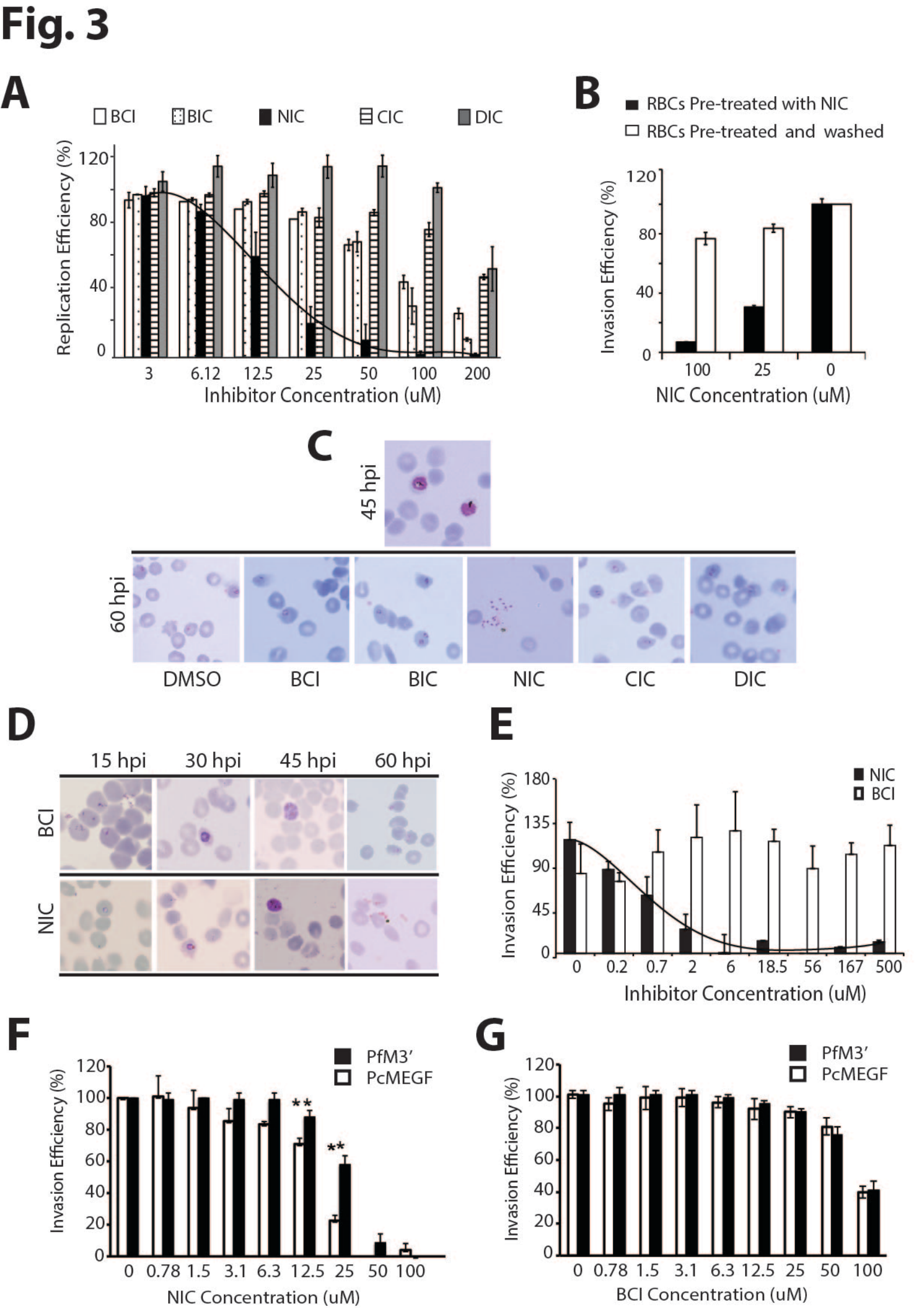
A
BCI
BIC
NIC
CIC
DIC
Replication Efficiency (%)
120
80
40
0
3
6.12
12.5
25
50
100
200
Inhibitor Concentration (uM)
B
RBCs Pre-treated with NIC
RBCs Pre-treated and washed
Invasion Efficiency (%)
120
80
40
0
100
25
0
NIC Concentration (uM)
C
45 hpi
60 hpi
DMSO
BCI
BIC
NIC
CIC
DIC
D
15 hpi
30 hpi
45 hpi
60 hpi
BCI
NIC
E
NIC
BCI
Invasion Efficiency (%)
180
135
90
45
0
0
0.2
0.7
2
6
18.5
56
167
500
Inhibitor Concentration (uM)
F
PfM3'
PcMEGF
Invasion Efficiency (%)
120
100
80
60
40
20
0
**
**
0
0.78
1.5
3.1
6.3
12.5
25
50
100
NIC Concentration (uM)
G
PfM3'
PcMEGF
Invasion Efficiency (%)
120
100
80
60
40
20
0
0
0.78
1.5
3.1
6.3
12.5
25
50
100
BCI Concentration (uM)

Fig. 4

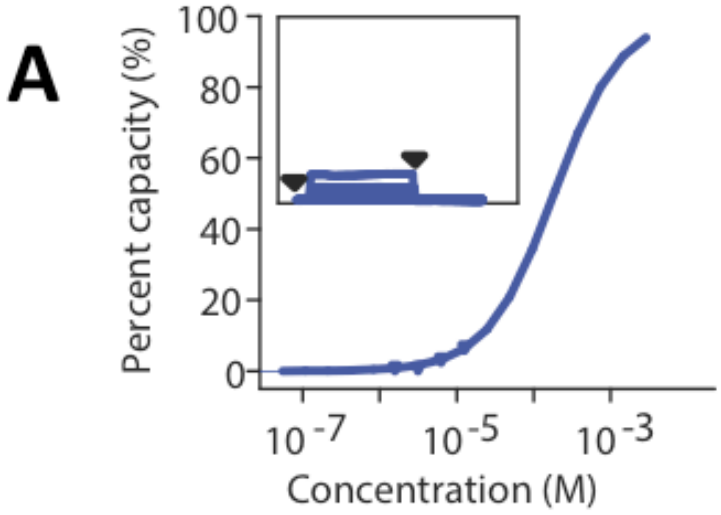
A
Percent capacity (%)
100
80
60
40
20
0
10^{-7}
10^{-5}
10^{-3}
Concentration (M)

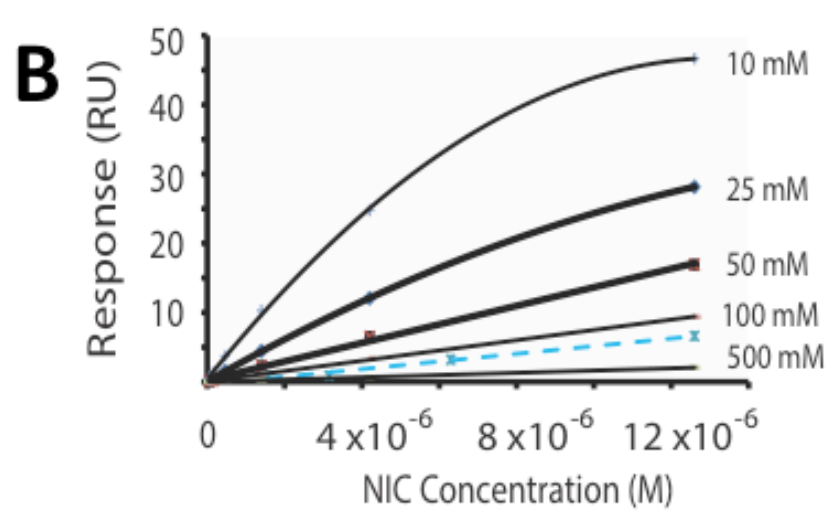
B
Response (RU)
50
40
30
20
10
10 mM
25 mM
50 mM
100 mM
500 mM
0
4×10^{-6}
8×10^{-6}
12×10^{-6}
NIC Concentration (M)

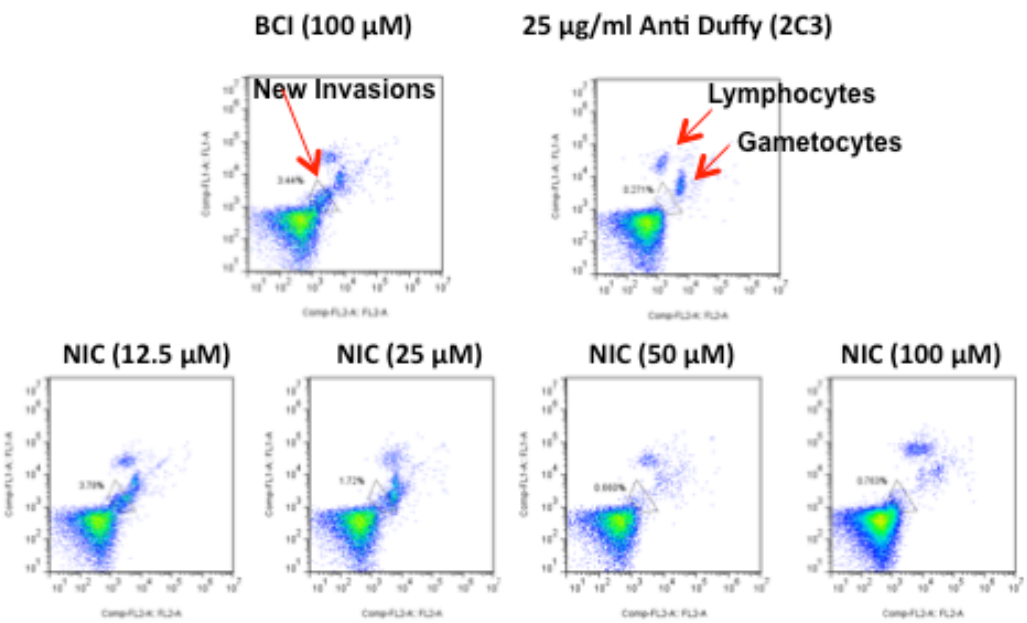
C
BCI (100 µM)
New Invasions
25 µg/ml Anti Duffy (2C3)
Lymphocytes
Gametocytes
NIC (12.5 µM)
NIC (25 µM)
NIC (50 µM)
NIC (100 µM)

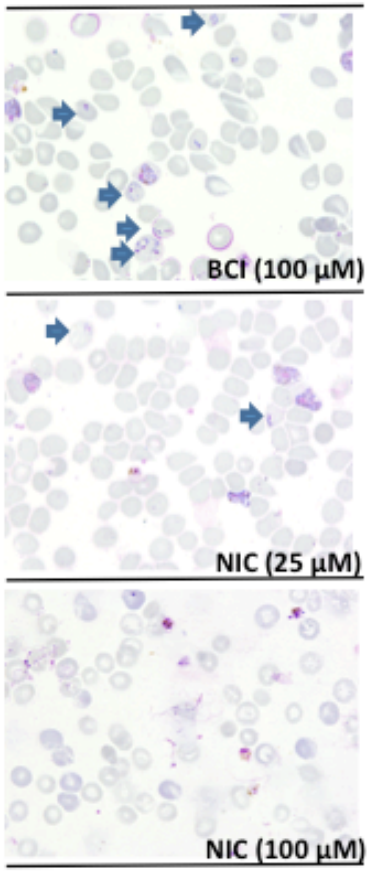
D
BCI (100 µM)
NIC (25 µM)
NIC (100 µM)

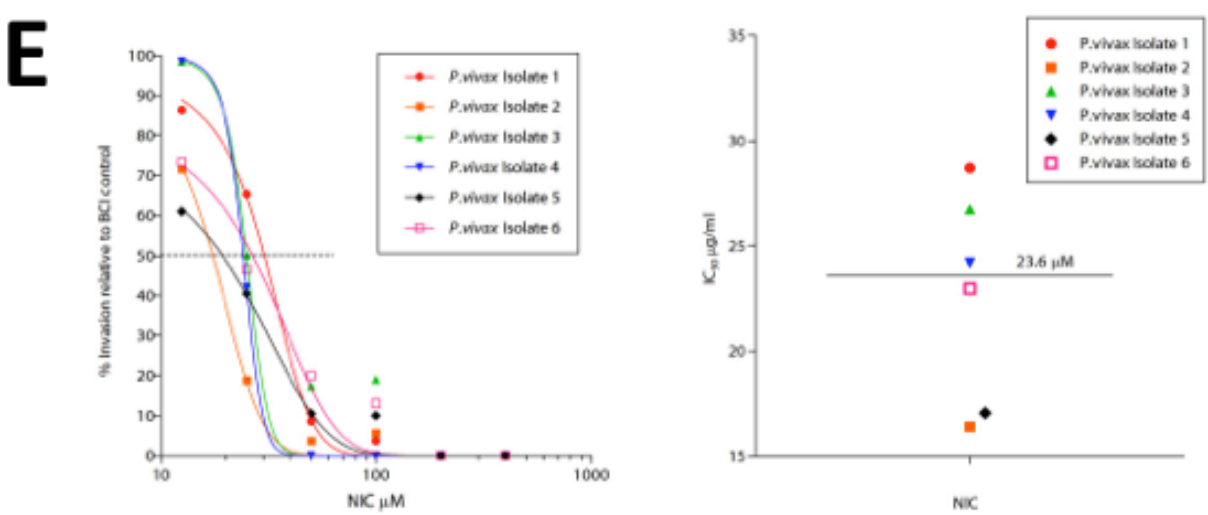
E
% Invasion relative to BCI control
NIC µM
P.vivax Isolate 1
P.vivax Isolate 2
P.vivax Isolate 3
P.vivax Isolate 4
P.vivax Isolate 5
P.vivax Isolate 6
23.6 µM
NIC

Table.1

Ligand	MW	-PLP1[a]	-PLP2	LigScore1	LigScore2	Jain	-PMF[b]	-LIE[c]	Dock Score
NIC	321.7	82.9	65.0	2.6	1.2	-0.3	36.0	1.4	45.0
CIC	339.2	46.4	46.7	1.9	3.2	0.6	27.1	-3.4	33.5
BIC	415.7	58.0	43.1	1.3	4.1	-1.9	55.9	-1.3	37.6
DIC	283.7	66.5	71.6	2.4	3.2	3.3	-18.0	-	27.6
KI-105	379.3	55.6	42.3	1.1	3.9	2.4	44.6	-2.1	38.6
DMBO	373.4	-	-	-	-	-	-	-	-

(Abbreviations: PLP1: Piecewise Linear Potential 1, **PLP2**: Piecewise Linear Potential 2, **LigScore1 & 2**: (fast, simple, scoring function for predicting receptor-ligand binding affinities), **Jain**: empirical scoring function through an evaluation of the structures and binding affinities of a series of protein-ligand complexes, **PMF**: Potential of Mean Force, LIE: ligand internal energy, **DS**: Dock Score)

Table. 2

Parasite Strains	IC50 (μM)	
	BCI	NIC
3D7	>200	21.7 ± 6.2
Dd2	>200	21.0 ± 0.1
FCR3	>200	20.0 ± 0.4
K1	>200	22.5 ± 6.5
T994	>200	23.6 ± 2.4
W2-mef	>200	21.6 ± 8.3
W2-mef (NM)	>200	22.3 ± 6.6